

Derivatives and Constraints in Chaotic Flows: Asymptotic Behaviour and a Numerical Method

Jean-Luc Thieault

Department of Applied Physics and Applied Mathematics
Columbia University, New York, NY 10027, USA

E-mail: jeanluc@mailaps.org

Abstract.

In a smooth flow, the leading-order response of trajectories to infinitesimal perturbations in their initial conditions is described by the finite-time Lyapunov exponents and associated characteristic directions of stretching. We give a description of the second-order response to perturbations in terms of Lagrangian derivatives of the exponents and characteristic directions. These derivatives are related to generalised Lyapunov exponents, which describe deformations of phase-space elements beyond ellipsoidal. When the flow is chaotic, care must be taken in evaluating the derivatives because of the exponential discrepancy in scale along the different characteristic directions. Two matrix decomposition methods are used to isolate the directions of stretching, the first appropriate in finding the asymptotic behaviour of the derivatives analytically, the second better suited to numerical evaluation. The derivatives are shown to satisfy differential constraints that are realised with exponential accuracy in time. With a suitable reinterpretation, the results of the paper are shown to apply to the Eulerian framework as well.

PACS numbers: 05.45.-a, 47.52.+j

Submitted to: Physica D

1. Introduction

We consider a collection of coupled ordinary differential equations (ODEs) associated with a vector field [1] (a continuous-time dynamical system). The general solution to these equations defines a flow mapping from the phase-space domain onto itself. For smooth vector fields, the flow can be regarded as a smooth coordinate transformation (a diffeomorphism) from the set of initial conditions to the state of the system at some later time [2, p. 276]. The coordinates describing the initial conditions are called the

^z In the mathematics literature the term flow is reserved for autonomous systems, the term transformation being preferred for the solutions generated by time-dependent vector fields [2, p. 96]. Because of the compelling nature of the fluid analogy, flow will be used in the more general sense in this paper.

Lagrangian coordinates, and those describing the state at a later time are called the Eulerian coordinates.

Generally, even a smooth vector field will lead to chaotic dynamics, with trajectories of nearby phase-space elements diverging rapidly from each other, at an average rate close to exponential for long times. The allowable rates are called the Lyapunov exponent of the flow [4], and are associated with characteristic directions of stretching. For chaotic flows, the transformation to Lagrangian coordinates becomes exceedingly contorted, and in practice it can no longer be inverted, due to the exponentially growing errors on the position of phase-space particles. Nevertheless, the presence of chaos can actually be advantageous because it leads to a large separation of time scales along the different characteristic directions of the flow. This separation of scale was used by Boozer [5], Tang and Boozer [6,7], and Giona and Adrover [8,9] to study fluid mixing and the dynamo problem.

Many equations of fluid dynamics are "advective" in nature, in that they describe the motion of a scalar or vector field as it is dragged by a flow, and possibly influenced by other effects such as diffusion and sources. Examples are the scalar advection-diffusion equation [10] and the induction equation for a magnetic field [11]. When expressed in Lagrangian coordinates, the advective term drops out of these types of equations. For scalar and vector advection-diffusion equations, one is left with a diffusion equation with anisotropic diffusivity. The anisotropic diffusivity arises because the Jacobian of the transformation between Lagrangian and Eulerian coordinates is not orthogonal. In a chaotic flow, the complexity of the transformation leads to a singular Jacobian, which is reflected in an exponentially-growing diffusivity that enhances mixing [6,12].

In Refs. [6,12], the singular Jacobian is decomposed to isolate the dominant direction of enhanced diffusion, leading to an expression in terms of the finite-time Lyapunov exponents and characteristic directions of stretching. To get a full solution of the advection-diffusion problem, the Lagrangian derivatives of the finite-time Lyapunov exponents and of the characteristic directions are needed. This is because the Lagrangian coordinate frame is position-dependent, so when derivatives of vector fields are taken one must also differentiate the basis vectors themselves (this is the same procedure as in covariant differentiation, or when fictitious forces appear after transforming to a rotating frame). Thus the necessity of obtaining Lagrangian derivatives of the vectors defining the coordinate frame. Because Lagrangian coordinates are also stretched with respect to Eulerian coordinates, the derivatives of the characteristic rates of separations (as characterised by the finite-time Lyapunov exponents) are also needed.

The problem of finding the asymptotic form of Lagrangian derivatives of the coordinate transformation induced by a flow has been addressed previously by Dressler and Farmer [13] and Taylor [14] in a different context. They examined the asymptotic behaviour of the Hessian, the quadratic form consisting of the second derivatives of the flow. The Hessian is the term that follows the Jacobian matrix in a Taylor expansion

Important exceptions are 1D vector fields, and 2D autonomous vector fields [3]. There are also other, more restricted classes of nonchaotic vector fields.

of the coordinate transformation from Lagrangian to Eulerian coordinates. Dressler and Farmer call the growth rates of the Hessian generalised or higher-order Lyapunov exponents. Their motivation lay in characterising the growth of nonlinear distortions of geometric quantities evolving under the influence of one-dimensional maps. The Lyapunov exponents quantify the leading order stretching of an infinitesimal ellipse moving with the phase fluid, and the generalised exponents describe deviations from an elliptical shape. Dressler and Farmer provided numerical results only for the largest Lyapunov exponent, because no numerical method exist to evolve the Hessian in a numerically stable manner that is not susceptible to limited precision. We provide such a method here.

In the Eulerian picture, the higher-order exponents also characterise the growth of extrinsic curvature of curves and surfaces embedded in a flow (material lines and surfaces), and so can be connected to work describing the evolution of the curvature of material lines in turbulent flows that originated with Batchelor [15{19], and more recently was applied to chaotic flows [20{22]. Our results derived in the Lagrangian frame can easily be adapted to the Eulerian picture, and provide a comprehensive view of second-order deformation processes in chaotic flows. The connexion between the Eulerian and Lagrangian pictures is made in an appendix.

Our approach is similar to Refs. [13,14] but is more general and applies to flows rather than maps: we aim to give estimates of the asymptotic growth rates of the Lagrangian derivatives of finite-time Lyapunov exponents and characteristic directions by appealing to arguments of "genericity" of the quantities involved, thus showing that the estimates will hold in essentially all cases. These arguments are formal in nature, in the sense that they do not provide a mathematical proof of the results, since there will always exist flows that can be specially chosen to violate any of the estimates. In particular, there could be flows with degenerate Lyapunov exponents (finite-time Lyapunov exponents that are degenerate for short periods of time do not concern us). We expect that even for degenerate exponents the results of the paper are applicable in a limited form. In practice the asymptotic behaviour holds to great accuracy for all flows examined. This will be verified in the numerical section of the paper.

To obtain the estimates of asymptotic behaviour of derivatives, we perform a singular value decomposition (SVD) of the tangent mapping of the flow, and differentiate the ODEs derived by Greene and Kim [23] directly. A careful analysis of the equations, with the assumption of a nondegenerate spectrum and a bounded attractor as in Goldhirsch et al. [24], leads to our asymptotic forms. We find that the Lagrangian derivatives along diverging directions of the finite-time Lyapunov exponents grow exponentially at the characteristic rate of that direction. This is consistent with the intuitive notion that small displacements in those directions will be exponentially amplified, so one expects derivatives to grow as well. For contracting directions, the opposite is true: the Lagrangian derivatives converge exponentially to time-asymptotic values, but often do so at a slower rate than the characteristic rate. The Lagrangian derivatives of the characteristic directions of stretching have a more complicated

behaviour, and it is not always true that a derivative along an expanding direction will diverge| the intuitive picture fails.

The asymptotic behaviour derived using the SVD method can be used to recover so-called differential constraints on the finite-time Lyapunov exponents and characteristic directions. Such constraints were first derived in two dimensions by Tang and Boozer [6] and Giona and Adrover [8] and were later extended to three dimensions by Thiéault and Boozer [25]. These earlier derivations provided limited results and were difficult to generalise to higher dimensions. In particular, the convergence rate of the constraints was not obtained, making it difficult to gauge their effect in approximations. The derivation given here overcomes these difficulties.

Whilst the SVD method is transparent and useful for theoretical derivations and interpretation, it is not well-suited for numerical purposes [26]: it possesses troubling singularities and involves a needlessly large number of equations to evolve. A better method is the QR decomposition [24,26], also known as the continuous Gram-Schmidt orthonormalisation method because it is a time-continuous version of earlier methods that involved re-orthonormalising a set of vectors evolved using the tangent map of the flow [3,27,28]. As for the SVD method, we adapt the QR method to finding the Lagrangian derivatives of the finite-time Lyapunov exponents and of the characteristic eigenvectors. The QR method can be used to verify the differential constraints mentioned above, since they depend on delicate cancellations that require the high accuracy afforded by the method herein in order to be convincingly established.

The outline of the paper is as follows. In section 2 we introduce the basic framework and notation necessary to the subsequent development. The central object of study is the metric tensor transformed to Lagrangian coordinates, and its diagonal form that contains all the information on the characteristic separations and directions. Section 3 describes the direct method of evolving the Hessian, where its governing equations are obtained by a variation of the ODEs and integrated directly. This method is not very useful numerically because the exponential blow up of the elements of the Hessian leads to issues of limited precision, but illustrates the basic principles and can be used to check the results of more complex methods, for short times.

A more powerful method is introduced in section 4, the SVD decomposition method. This allows derivation of the asymptotic behaviour of the Lagrangian derivatives. The asymptotic behaviour is exploited in section 5 to investigate the properties of the Hessian, and to give a new and powerful derivation of differential constraints in chaotic flows.

In section 6 the QR decomposition is used to develop a suitable numerical method for evolving the various Lagrangian derivatives. The numerical method is then used to verify to high precision the geometrical constraints derived in section 5. Section 7 consists of a brief summary of the main results of this paper and of possible future work, as well as a discussion of possible applications.

2. Characteristic Directions of Trajectory Separation

We begin with a brief overview of the concepts and notation we shall use. We consider the n -dimensional dynamical system

$$\dot{\mathbf{x}} = \mathbf{v}(\mathbf{x}; t); \quad (2.1)$$

where the overdot indicates a time derivative, and \mathbf{v} is a smooth function of \mathbf{x} and t . The solution to (2.1) is a function $\mathbf{x}(t)$, with initial condition $\mathbf{x}(t_0) = \mathbf{a}$. We can thus regard $\mathbf{x}(t)$ as a coordinate transformation from the set of initial conditions \mathbf{a} to the state at time t ; we write this transformation explicitly as $\mathbf{x}(\mathbf{a}; t)$. Following standard terminology, we call \mathbf{x} the Eulerian coordinates and \mathbf{a} the Lagrangian coordinates.

The time-evolution of the Jacobian matrix $M_p^i \equiv \partial x^i / \partial a^p$ is given by

$$\dot{M}_p^i = \sum_{j=1}^n G^i_j M_p^j; \quad (2.2)$$

where $G^i_j \equiv \partial v^i / \partial x^j$; the initial conditions are $M_p^i = \delta_p^i$, since the coordinates \mathbf{x} and \mathbf{a} initially coincide. The nonsingular Jacobian matrix tells us how to transform vectors in \mathbf{a} coordinates to vectors in \mathbf{x} coordinates (M_p^i is the tangent mapping to the transformation $\mathbf{x}(\mathbf{a}; t)$). Now construct the matrix

$$g_{pq} \equiv \sum_{i=1}^n M_p^i M_q^i; \quad (2.3)$$

called the metric tensor in Lagrangian coordinates or Cauchy-Green strain tensor [29]; it is symmetric and positive-definite, so it can be diagonalized with real positive eigenvalues and orthogonal eigenvectors and rewritten as

$$g_{pq} = \sum_{i=1}^n \lambda_i^2 (\hat{e}_i)_p (\hat{e}_i)_q; \quad (2.4)$$

with $\hat{e}_i(\mathbf{a}; t)$ and $\lambda_i^2(\mathbf{a}; t)$ respectively the i th eigenvector of $g_{pq}(\mathbf{a}; t)$ and corresponding eigenvalue. We refer to the λ_i as the coefficients of expansion, because they represent the relative deformation of the principal axes of an infinitesimal ellipsoid carried by the flow. The coefficients of expansion can be used to define the finite-time Lyapunov exponents,

$$\lambda_i(\mathbf{a}; t) \equiv \frac{1}{t} \log \lambda_i(\mathbf{a}; t); \quad (2.5)$$

The finite-time Lyapunov exponents, $\lambda_i(\mathbf{a}; t)$ describe the instantaneous average rate of exponential separation of neighbouring trajectories. The multiplicative ergodic theorem of Oseledec [30] implies that the infinite-time limit $\lim_{t \rightarrow \infty} \lambda_i(\mathbf{a}; t)$ exists and is independent of the initial condition \mathbf{a} in a given ergodic domain, for almost all initial conditions. The infinite-time limit $\lim_{t \rightarrow \infty} \hat{e}_i(\mathbf{a})$ of the characteristic eigenvectors $\hat{e}_i(\mathbf{a}; t)$ also exists but depends on the initial condition. The Lyapunov exponents converge very slowly, whereas for nondegenerate exponents the characteristic eigenvectors converge

To lighten the notation, we omit the explicit dependence of \mathbf{x} on the initial time t_0 .

We are implicitly assuming the Euclidean norm for vectors in Eulerian space.

exponentially fast [24]. The slow convergence of the Lyapunov exponents indicates that the instantaneous separation rate of neighbouring trajectories is not at all exponential on a typical attractor; only in the infinite-time limit do the trajectories show a mean exponential rate of separation. The instantaneous deviations from this exponential rate are very large. However, even though it may not be growing exponentially, an eigenvalue associated with a positive Lyapunov exponent becomes very large after a relatively short time, and conversely an eigenvalue associated with a negative Lyapunov exponent becomes very small. It is thus an abuse of language, but a convenient one we shall use, to refer to the λ_i 's as growing or shrinking exponentially.

In this paper we shall assume that the eigenvalues λ_i are nondegenerate and ordered such that $\lambda_1 > \dots$. After allowing some time for chaotic behaviour to set in, we have that $\lambda_i > 0$ for $i < n/2$. We shall make use of this ordering often in the subsequent development.

3. Lagrangian Derivatives: Direct Method

When the vector field $v(x;t)$ is a known analytic function, explicit evolution equations for the spatial derivatives of the \hat{e}_i and \hat{e} can be derived, as pointed out in Refs. [6] and [31]. The method involves expressing the derivatives of \hat{e}_i and \hat{e} in terms of derivatives of the metric tensor g . This is done by taking the Lagrangian derivative of the diagonal form (2.4) of g and dotting the resulting expression with the eigenvectors \hat{e}_i . We obtain

$$\frac{\partial (\hat{e}_i)_q}{\partial a^p} = \sum_{r,s} \frac{1}{2} (\hat{e}_i)_r (\hat{e}_i)_s (\hat{e}_i)_q \frac{\partial g_{rs}}{\partial a^p}; \quad (3.1)$$

$$\frac{\partial \hat{e}}{\partial a^p} = \frac{1}{2} \sum_{r,s} (\hat{e})_r (\hat{e})_s \frac{\partial g_{rs}}{\partial a^p}; \quad (3.2)$$

The derivatives of the metric are obtained from the Hessian $K_{qr}^k \equiv \partial^2 x^k / \partial a^q \partial a^r$ of the coordinate transformation via the relation

$$\frac{\partial g_{pq}}{\partial a^r} = \sum_{i=1}^{X^n} M_i^p K_{qr}^i + M_i^q K_{pr}^i; \quad (3.3)$$

obtained by differentiating the non-diagonal form (2.3) of g . The Hessian is symmetric in its lower indices, and it is computed by solving the evolution equation

$$K_{qr}^k = \sum_{i=1}^{X^n} G_i^k K_{qr}^i + \sum_{i,j=1}^{X^n} X_{ij}^k M_i^q M_j^r; \quad (3.3)$$

where $X_{ij}^k \equiv \partial^2 v^k / \partial x^i \partial x^j$. For the existence and uniqueness of solutions to (3.3), it is necessary that $\partial^2 v^k / \partial x^i \partial x^j$ be Lipschitz, but it is sufficient that v be at least thrice-differentiable. Equation (3.3) is obtained by differentiating (2.2), and the initial condition is $K = 0$. The time derivatives (the overdots) are taken at constant a , so they can be computed with Lagrangian derivatives.

The linear part of (3.3) is the same as for (2.2), but now there is a nonlinear coupling term to M . Since for a chaotic flow the matrix M has at least one exponentially growing

eigenvalue, the elements of the Hessian K typically grow faster than M , owing to the nonlinear coupling. Numerically, the system (3.3) is thus unstable in an essential way, and we can expect the integration to give meaningless results (except along the dominant stretching direction) after the elements of K become too large. Nevertheless, if one is not interested in long-time behaviour the direct method can yield satisfactory results. It is not suitable for a detailed, accurate, long-time solution of the Lagrangian derivatives. We develop such methods in sections 4 and 6.

4. Asymptotic Behaviour using the SVD Method

4.1. Basic Method

Any matrix, and in particular the Jacobian matrix M , can be decomposed into the product

$$M = U F V^T; \quad (4.1)$$

where U and V are orthogonal matrices and F is diagonal. The superscript T denotes a matrix transpose. This decomposition is called the singular value decomposition (SVD), and is unique up to permutations of rows and columns. The diagonal elements of F are called the singular values. Requiring that the singular values be ordered decreasing in size makes the decomposition unique (for nondegenerate eigenvalues). As can be seen by substitution of (4.1) into (2.3), the columns of V are eigenvectors of g , $V_q = (\hat{e})_q$, with eigenvalues given by the diagonal elements of $F^T F$, $(F^T F)_{qq} = \sigma_q^2$. The advantage of the SVD is that it separates neatly the parts of M that are growing or shrinking exponentially in size (as determined by the coefficients of expansion σ_q). The SVD has the following interpretation: if we consider an infinitesimally small "ball" of initial condition obeying (2.1), it will deform into an ellipsoid under the action of the flow. The σ_q give the relative stretching of each principal axis of the ellipsoid, the orthogonal matrix V gives the principal axes of stretching in Lagrangian coordinate space, and the orthogonal matrix U gives the absolute orientation of the ellipse in Eulerian space. Constructing the metric tensor as in (2.3) eliminates the Eulerian orientation, retaining the essential features of the stretching.

Greene and Kim [23] derived the equations satisfied by U , V , and F :

$$\dot{U} = \mathcal{G} U; \quad (4.2)$$

$$(U^T U) = \begin{cases} \frac{\mathcal{G}_{qq}^2 + \mathcal{G}_{pp}^2}{2} & \text{for } q \neq p; \\ 0 & \text{for } q = p; \end{cases} \quad (4.3)$$

$$(V^T V) = \begin{cases} \frac{\mathcal{A}_{qq}^2}{2} & \text{for } q \neq p; \\ 0 & \text{for } q = p; \end{cases} \quad (4.4)$$

where

$$\mathcal{G} \equiv U^T G U; \quad \mathcal{A} \equiv \mathcal{G} + \mathcal{G}^T;$$

Numerically, the SVD method has limitations: the number of quantities to evolve is large, and when $t \rightarrow +\infty$ the denominators become singular (See Refs. [23,26] for a discussion of these issues). However, conceptually the method is very straightforward and transparent, and it gives explicit equations for all the quantities we are interested in, as opposed to the QR method (section 6) which needs to be corrected to yield the true value of the λ .

For large time, when $t \rightarrow +\infty$, $\lambda_i \rightarrow 0$, we can approximate (4.3) and (4.4) by

$$\begin{aligned} (U^T U)_{ij} &= \frac{1}{\lambda_i + \lambda_j} < 0; & (V^T V)_{ij} &= \frac{1}{\lambda_i + \lambda_j} < 0; \\ (U^T U)_{ii} &= \frac{1}{2\lambda_i} > 0; & (V^T V)_{ii} &= \frac{1}{2\lambda_i} > 0; \\ (U^T U)_{ij} &= 0 & (V^T V)_{ij} &= 0. \end{aligned} \quad (4.5)$$

where we have used

$$\begin{aligned} \lambda_i &= -\frac{1}{2} \text{Tr}(U^T U)_{ii} < 0; \\ \lambda_i &= -\frac{1}{2} \text{Tr}(V^T V)_{ii} < 0; \\ \lambda_i &= \max_j \left| \frac{\text{Tr}(U^T U)_{ij}}{\lambda_j} \right| > 0. \end{aligned} \quad (4.6)$$

The matrix Λ is symmetric, and defined such that (for nondegenerate λ) all of its elements are decaying exponentially. Because of the ordering of the λ , the diagonal element Λ_{ii} represents the element on the i th row or column that decays the slowest, that is, $\Lambda_{ii} = \max_j \lambda_j$.

If we assume that the evolution of the system takes place on some bounded domain, then we know that G , and hence \dot{G} and \dot{A} , remains bounded (we also assume that the vector field v is smooth). Thus, the right-hand side of $V^T \dot{V}$ in (4.5) goes to zero exponentially, and we can solve the equation perturbatively for large time,

$$V_q = V_q^1 + \int_{t_0}^t V_q^1 (V^T \dot{V}) dt + O(t^{-2})$$

for some constant V_q^1 , which can only be determined by solving the unapproximated equation (4.4). We conclude that for large t the matrix V has the form [24]

$$V_q = \hat{V}_q + V_q^1; \quad t \rightarrow +\infty \quad (4.7)$$

Since $V_q = (\dot{e})_q$ and $\dot{e} \rightarrow 0$, the characteristic eigenvectors converge exponentially to their time-asymptotic value, $(\dot{e}^1)_q = V_q^1$. The elements of the matrix U do not in general converge. The Lyapunov exponents have a very slow (logarithmic) convergence which does not concern us here, as we are considering timescales of fast (roughly exponential) convergence.

4.2. Lagrangian Derivatives

Having derived the equations of motion for the SVD of M , we can now take the Lagrangian derivative of these equations of motion, in a manner analogous to section 3. We define the quantities

$$\begin{aligned} \dot{V}_q &= \sum_q V_q \frac{\partial \log}{\partial a^q}; & \dot{U}_i &= \sum_{q,i} V_q U_i \frac{\partial U_i}{\partial a^q}; & \dot{V}_p &= \sum_{q,p} V_q V_p \frac{\partial V_p}{\partial a^q}; \end{aligned} \quad (4.8)$$

which are simply the Lagrangian derivatives of \mathbf{U}_i , and V_p expressed in a convenient frame. Note that $\mathbf{U}_i = \mathbf{U}_i$ and $V_p = V_p$. The Lagrangian derivatives may be regarded as the components of the curvature of the vector fields defined by the columns of V_p . From (4.2)–(4.4), we can find equations for the evolution of \mathbf{U}_i , V_p , and \mathbf{X} ,

$$\dot{\mathbf{U}}_i = \mathbf{X}^T (\mathbf{V}^T \mathbf{V}) \mathbf{U}_i + \mathbf{X}^T \mathbf{A} \mathbf{U}_i + \mathbf{X}^T \mathbf{X} \mathbf{U}_i; \quad (4.9)$$

$$\begin{aligned} \dot{V}_p &= \mathbf{X}^T \mathbf{h}^T (\mathbf{V}^T \mathbf{V}) \mathbf{U}_i + (\mathbf{U}^T \mathbf{U}) \mathbf{V}_p + (\mathbf{U}^T \mathbf{U}) \mathbf{V}_p \\ &\quad + \mathbf{X}^T V_q \frac{\partial}{\partial a^q} (\mathbf{U}^T \mathbf{U}) \mathbf{U}_i; \end{aligned} \quad (4.10)$$

$$\begin{aligned} \dot{\mathbf{X}} &= \mathbf{X}^T \mathbf{h}^T (\mathbf{V}^T \mathbf{V}) \mathbf{U}_i + (\mathbf{V}^T \mathbf{V}) \mathbf{X} + (\mathbf{V}^T \mathbf{V}) \mathbf{X} \\ &\quad + \mathbf{X}^T V_q \frac{\partial}{\partial a^q} (\mathbf{V}^T \mathbf{V}) \mathbf{U}_i; \end{aligned} \quad (4.11)$$

where

$$\mathbf{X} = \sum_{k,i,j} U_k U_i U_j \frac{\partial^2 V^k}{\partial x^i \partial x^j}, \quad (4.12)$$

is symmetric in i and j .

In Appendix A, the asymptotic behaviour of the derivatives is obtained from the equations of motion (4.9)–(4.11). We now summarise the main results of that section: for $t \gg 1$, by which we mean that the dynamical system has evolved long enough for the quantities \mathbf{U}_i to have reached a regime of quasi-exponential behaviour, we have that the Lagrangian derivatives defined by (4.8) evolve asymptotically as

$$\dot{\mathbf{U}}_i = \max(\lambda_i; 0) e^{\lambda_i t} \mathbf{U}_i; \quad (4.13)$$

$$\dot{V}_p = \max(\lambda_p; 0) e^{\lambda_p t} V_p + \max(\lambda_p; 1) e^{\lambda_p t} V_p; \quad (4.14)$$

$$\dot{\mathbf{X}} = \max(\lambda_X; 0) e^{\lambda_X t} \mathbf{X} + \max(\lambda_X; 1) e^{\lambda_X t} \mathbf{X}; \quad (4.15)$$

Recall that in all these cases the first index, i , denotes the characteristic eigendirection $\hat{\mathbf{e}}_i$ along which the Lagrangian derivative is evaluated. For a given i with $\lambda_i > 0$, corresponding to an expanding direction of the flow, both \mathbf{U}_i and V_p grow exponentially with time (the constant λ_i is then irrelevant). Thus, Lagrangian derivatives of \log along an expanding direction become more singular with time, to a degree commensurate with the separation of neighbouring initial conditions along that direction, as given by (4.13).

Conversely, for i with $\lambda_i < 0$, corresponding to a contracting direction of the flow, both \mathbf{U}_i and V_p decrease exponentially with time, converging toward zero and \mathbf{X} converging to a constant, λ_i . The convergence rate of both these quantities, however, is not necessarily equal to $|\lambda_i|$ but may be slower (though still converging), as denoted by the \max in (4.13) and (4.14). This slower convergence rate of \mathbf{X} has two sources: (i) From (4.7), the V in the definition (4.8) of \mathbf{X} converges at a rate $|\lambda_V|$; (ii) The term in (4.9) limits the convergence to λ_i .

The interpretation of the long-time behaviour of Lagrangian derivatives of V , the characteristic eigenvectors, is less generic. For a contracting direction, the derivatives converge to the constant value 1 at a rate of $\max(\lambda_1, \lambda_2)$. This convergence rate is dominated by the convergence of the individual V 's in (4.8), as given by (4.7). For an expanding direction, the specific behaviour of \dot{V} depends on the relative magnitudes of the coefficients of expansion. However, for a non-contracting direction it is always true that

$$(\dot{V} \cdot V) \geq 1;$$

so the gradients of \hat{e} along expanding directions grow much more slowly than those of $\log \hat{e}$.

We close this section by considering the asymptotic behaviour of the Lagrangian derivative of the determinant, $\det g$, of the metric tensor g . From (2.4),

$$\det g = \sum_{j=1}^N V_j^2;$$

so that the Lagrangian derivative of the determinant along V is

$$\dot{\det g} = \sum_q V_q \frac{\partial}{\partial a^q} \log \det g = \sum_q \dot{V}_q \quad (4.16)$$

An equation of motion for \dot{V} is obtained by summing (4.9) over j , yielding

$$-\dot{V} = \sum (V^T V) + \sum \dot{V} \quad (4.17)$$

where the \dot{V} term has dropped out. The term $\sum \dot{V}$ is proportional to $\text{tr} \dot{V}$, so for an incompressible flow the solution to (4.17) is $\dot{V} = 0$. But in general, for a compressible flow with non-uniform $\text{tr} \dot{V}$, we find

$$\dot{V} = \max(\lambda_1, \lambda_2) e^{\lambda_1 t} + 1; \quad t \geq 1; \quad (4.18)$$

where the time dependence of $e^{\lambda_1 t}$ is non-exponential. In contrast to (4.18), the limiting rate in (4.18) is due entirely to the convergence rate of V , as given by (4.7).

5. Properties of the Hessian and Constraints

5.1. Symmetry of the Hessian

We now make contact with the work of Dressler and Farmer [13] and Taylor [14] on the form of the generalised Lyapunov exponents, which describe the asymptotic behaviour of the Hessian. The Hessian, defined in section 3, can be recovered from the Lagrangian derivatives of section 4.2. Following Dressler and Farmer [13], we project the components of the Hessian onto the U and V bases and define

$$K_{pq} = \sum U_p \cdot \dot{V}_q \quad (5.1)$$

Writing $K_{pq} = \partial M_p / \partial a^q$, and using the SVD decomposition (4.1) for M , we find

$$K = \dots + \dots + \dots \quad (5.2)$$

The asymptotic behaviour of the Hessian is easily derived from (4.13), (4.14), and (4.15),

$$\mathbb{K} = \max(\dots) \mathbb{K}^{\frac{1}{2}}; \quad (5.3)$$

where $\mathbb{K}^{\frac{1}{2}}$ is a non-exponential function, as found for maps in Refs. [13,14].

Since the Hessian is symmetric in its lower indices, we could have equally well written

$$\mathbb{K} = \dots + \dots; \quad (5.4)$$

where we simply interchanged and in (5.2). Equating (5.2) and (5.4), we find the relations

$$(\dots + \dots) = \dots; \quad (5.5)$$

$$(\dots) = \dots; \quad (5.6)$$

Equation (5.5) defines $n(n-1)$ independent relations, whilst (5.6) defines $n(n-1)(n-2)/2$ relations. Thus, a total of $n^2(n-1)/2$ quantities are dependent on the others and can be eliminated, which is exactly the number of dependent components of \mathbb{K} . The relation (5.6) can be solved for to yield

$$= \frac{1}{2} \dots + \dots + \dots + \dots; \quad (5.7)$$

when \dots , \dots , and \dots differ. Similarly, (5.5) can trivially be solved for \dots . Equations (5.5) and (5.7) express all of the \dots in terms of the \dots and \dots . However, the asymptotic behaviour of \dots cannot be recovered from these equations by simply substituting (4.13) and (4.14). The reason is that the asymptotic form (4.15) hinges on delicate cancellations between the \dots and \dots that are not manifest from simply looking at their equations of motion. For instance, in (5.7) the coefficient of each \dots term grows exponentially, even though some of the \dots 's have been shown to converge.

Although we are not using the SVD method to obtain numerical results, the considerations of this section also apply to the QR method of section 6. The relations (5.5) and (5.6) can then be used as a diagnostic tool to monitor the numerical results.

5.2. Differential Constraints

Rather than solving for the \dots , if the flow is chaotic the relations (5.5) and (5.6) can be put to good use in another manner. The Lagrangian derivatives of U , as contained in \dots , are not quantities of great interest to us. They describe the sensitive dependence on initial conditions of the absolute orientation of phase-uid elements in Eulerian space. This information is not necessary for solving problems in Lagrangian coordinates, and is too sensitive to initial conditions to be of use anyhow. We thus substitute the time-asymptotic form of \dots , given by (4.13), in the right-hand side of (5.5) and (5.6), yielding

$$+ \dots = \max \dots; \quad (5.8)$$

$$= \dots \max(\dots) e^{\dots} - \dots \max(\dots) e^{\dots}; \quad (5.9)$$

Table 1. The total number of type I constraints for low-dimensional systems, as given by (5.12). The rows denote n , the columns the number of contracting directions $m \leq n$.

	1	2	3	4	5	6	7
1	0						
2	1	1					
3	2	3	3				
4	3	5	6	6			
5	4	7	9	10	10		
6	5	9	12	14	15	15	
7	6	11	15	18	20	21	21

where, as before, λ_1, λ_2 , and λ_3 differ. Below we show that under certain conditions the right-hand side of (5.8) or (5.9) converges toward zero, giving us asymptotic differential constraints on $\dot{\mathbf{x}}$ and $\dot{\mathbf{y}}$.

5.2.1. Type I Constraints For $\lambda_i < 0$, (5.8) can be written

$$\dot{\mathbf{x}}_i + \dot{\mathbf{y}}_i = \max \left\{ \lambda_i^2 e^{-\lambda_i t}; \lambda_i \right\} < 0; \quad (5.10)$$

If the index i corresponds to a contracting direction ($\lambda_i < 0$), the right-hand side of (5.10) goes to zero exponentially fast, at a rate λ_i^2 or λ_i , whichever is slowest. In that case (5.10) is a constraint implying that for large t we have

$$(\dot{\mathbf{x}}_i + \dot{\mathbf{y}}_i) \neq 0; \quad \lambda_i < 0; \quad (5.11)$$

We refer to (5.11) as type I constraints. The total number of such constraints is

$$N_I = m \cdot n - \frac{1}{2} (m + 1); \quad (5.12)$$

where n is the dimension of the space and m is the number of contracting directions (i.e., the number of negative Lyapunov exponents) possessed by the flow in a particular ergodic domain. Table 1 gives the number of type I constraints, N_I , as a function of n and m .

In two dimensions, we typically have one contracting direction, so there is a single type I constraint. This is the same constraint that was derived in Refs. [6,25].

In three dimensions, for an autonomous flow, we typically also have one contracting direction. There are then two type I constraint. These constraints correspond to those derived in Ref. [25].

A special case of the type I constraints is obtained by setting $\lambda_i = n$ in (5.10), and then summing over $\lambda_i < n$, to yield

$$\sum_q \frac{1}{j!^{j=2}} \frac{\partial}{\partial a^q} \dot{\mathbf{y}}^{j=2} (\mathbf{e}_n)_q = \sum_q (\mathbf{e}_n)_q \frac{\partial}{\partial a^q} \log n - \max \left\{ n; \frac{2}{nn} \right\} \neq 0; \quad (5.13)$$

This constraint was discovered numerically and used by Tang and Boozer [6, 7, 31, 32] and derived in three dimensions by Thiéault and Boozer [25]. It has been used to study the anticorrelation between curvature and stretching [6, 25, 31] and to transform the advection-diffusion equation in Lagrangian coordinates to an approximate one-dimensional form [12]. (See also Appendix C for an Eulerian version of the constraint.) The present method not only gives the constraint in a very direct manner for any dimension n , but it also provides us with its asymptotic convergence rate, as determined by the right-hand side of (5.13). It also shows that the constraint (5.13) does not stand alone, but is the sum of several independent constraints. More details on the differences between this paper and earlier approaches are given in section 5.3.

5.2.2. Type II Constraints Equation (5.9) implies that

$$\max_{i,j} \left| \frac{\partial^2 \mathcal{L}}{\partial a^i \partial a^j} \right| \geq \frac{1}{2} \left(\frac{\partial \mathcal{L}}{\partial a^i} \right)^2 + \left(\frac{\partial \mathcal{L}}{\partial a^j} \right)^2 : \quad (5.14)$$

We are interested in finding constraints analogous to the type I constraints of section 5.2.1. It is clear that unless both α_i and α_j are greater than $\frac{1}{2}$, the right-hand side of (5.14) is of order unity or greater, and so does not go to zero. We can assume without loss of generality that $\alpha_i < \frac{1}{2}$, so that

$$\max_{i,j} \left(\alpha_i \alpha_j \right) < \frac{1}{4} < \frac{1}{2} ; \quad (5.15)$$

where we have used (5.10). Whether or not (5.15) is a constraint depends on the specific behaviour of $\alpha_i = \frac{1}{2} \frac{\partial \mathcal{L}}{\partial a^i}$. Clearly, we have a constraint if $\alpha_i > \frac{1}{2}$, since $\alpha_i > \frac{1}{2}$. This provides a lower bound on the number N_{II} of type II constraints; by choosing α_i from the m contracting directions, and summing over the remaining $n - m$ directions, we obtain

$$N_{II} \geq \frac{1}{2} m^2 - \frac{1}{2} (m+2)(n-m) = \frac{1}{2} m(m-1) : \quad (5.16)$$

But even if $\alpha_i < \frac{1}{2}$ we can have a constraint, as long as $\alpha_i > \frac{1}{2}$. This depends on the particular problem at hand; hence, (5.16) is only a lower bound, but a fairly tight one for low dimensions. Table 2 enumerates the minimum number of type II constraints as a function of n and m .

Note that when $\alpha_i < \frac{1}{2}$, and $\alpha_j > \frac{1}{2}$ we can write

$$\left(\frac{\partial \mathcal{L}}{\partial a^i} \right)^2 + \left(\frac{\partial \mathcal{L}}{\partial a^j} \right)^2 = \sum_p \left(\frac{\partial \mathcal{L}}{\partial a^p} \right)^2 \left(\frac{\partial \mathcal{L}}{\partial a^p} \right)^2 : \quad (5.17)$$

where the Lie bracket is

$$\left[\frac{\partial \mathcal{L}}{\partial a^i}, \frac{\partial \mathcal{L}}{\partial a^j} \right] = \sum_p \left(\frac{\partial \mathcal{L}}{\partial a^p} \right) \frac{\partial}{\partial a^p} \left(\frac{\partial \mathcal{L}}{\partial a^j} \right) - \sum_p \left(\frac{\partial \mathcal{L}}{\partial a^p} \right) \frac{\partial}{\partial a^p} \left(\frac{\partial \mathcal{L}}{\partial a^i} \right) : \quad (5.18)$$

The type II constraints are thus forcing certain Lie brackets of the characteristic directions \hat{e}_i to vanish asymptotically. The geometrical implications of this, and perhaps a connexion to the Frobenius theorem [33] and the existence of submanifolds, remains to be explored.

Table 2. Lower bound on the number of type II constraints, as given by (5.16). The rows denote n , the columns the number of contracting directions $m \leq n$.

	1	2	3	4	5	6	7
1	0						
2	0	0					
3	1	1	1				
4	3	4	4	4			
5	6	9	10	10	10		
6	10	16	19	20	20	20	
7	15	25	31	34	35	35	35

If we restrict to three dimensions, then there is at least one type II constraint; it can be written as

$$r_{231} - r_{321} = e_1 \cdot \nabla e_1; \quad (5.19)$$

where r_0 denotes a gradient with respect to the Lagrangian coordinates a . This constraint is the special case that was derived in Ref. [25].

5.3. Riemannian Curvature

We now compare the approach of section 5.2 to the earlier attempts of Refs. [6, 25], where the constraints were derived for two and three dimensional flows by examining the form of the Riemann curvature tensor associated with the metric g . We list the advantages of the present method.

Nontrivial metrics can have curvature; a straightforward method of computing that tensor is through the use of Ricci rotation coefficients [34],

$$\omega_{ij}^k = \sum_{\alpha} U_i U_j \frac{\partial}{\partial x^\alpha} U_k; \quad (5.20)$$

These satisfy the antisymmetry property $\omega_{ij}^k = -\omega_{ji}^k$, and can be rewritten in terms of the ω of (4.8) as

$$\omega_{ij}^k = \omega_{ij}^k{}^1; \quad (5.21)$$

In terms of the rotation coefficients, the Riemann curvature tensor is [34, p. 51]

$$R_{ijkl} = \sum_{\alpha} U_i \frac{\partial}{\partial x^\alpha} \omega_{jk}^\alpha - \sum_{\alpha} U_j \frac{\partial}{\partial x^\alpha} \omega_{ik}^\alpha + \sum_{\alpha} \omega_{ij}^\alpha \omega_{\alpha k}^l - \sum_{\alpha} \omega_{jk}^\alpha \omega_{\alpha i}^l; \quad (5.22)$$

If we use the relations (5.5) and (5.6) to solve for ω in terms of ω and ω , we can

Let

$$\mathbf{R} = \mathbf{Q} \mathbf{D} \mathbf{Q}^T; \quad \mathbf{D} = \text{diag}(\lambda_1, \dots, \lambda_n); \quad \mathbf{R}_q = \mathbf{D} \mathbf{r}_q; \quad (6.2)$$

That is, \mathbf{R} is a vector containing the diagonal elements of \mathbf{R} , \mathbf{D} is a diagonal matrix with the λ_i along the diagonal, and \mathbf{r} is \mathbf{R} with the i th row rescaled by λ_i . The time-evolution of these quantities is [24,26]

$$\dot{\mathbf{R}} = \mathbf{G} \mathbf{R}; \quad (6.3)$$

$$\begin{aligned} \dot{(\mathbf{Q}^T \mathbf{Q})} &= \mathbf{G} + \mathbf{G}^T; \\ \dot{\mathbf{D}} &= \mathbf{D} \mathbf{A} \mathbf{D}; \end{aligned} \quad (6.4)$$

$$\dot{\mathbf{r}}_q = \mathbf{X}^q \mathbf{r}_q - \mathbf{A} \mathbf{r}_q; \quad (6.5)$$

where

$$\mathbf{G} = \mathbf{Q}^T \mathbf{G} \mathbf{Q}; \quad \mathbf{A} = \mathbf{G} + \mathbf{G}^T; \quad (6.6)$$

Equation (6.3) is identical to (4.2) for \mathbf{R} in the SVD method, and (6.4) is identical to the time-asymptotic form of (4.3) for \mathbf{U} , given by (4.5). Hence, we expect \mathbf{R} and \mathbf{U} to have similar asymptotic behaviour, though their exact values differ.

Unlike the SVD method, in the QR method the eigenvalues λ_i and eigenvectors $\hat{\mathbf{e}}_i$ are not evolved directly. They can be recovered from the \mathbf{D} and the matrix \mathbf{r} in the following manner. Let \mathbf{d} be the lower-triangular matrix that effects the Gram-Schmidt orthonormalisation of \mathbf{r} , that is

$$\mathbf{W}_q = \mathbf{d} \mathbf{r}_q; \quad (6.7)$$

where $d_{ii} = 0$ for $i < j$, and \mathbf{W} is orthogonal. The eigenvectors of \mathbf{g} and corresponding coefficients of expansion are then

$$(\hat{\mathbf{e}})_q = \mathbf{W}_q; \quad \mathbf{c} = \frac{\mathbf{R}}{\mathbf{d}}; \quad (6.8)$$

to exponential accuracy with time (the relative error on $\hat{\mathbf{e}}$ and \mathbf{c}^2 is of order $(\epsilon = \epsilon_1)^2$). Equation (6.8) is proved in Appendix B.

By definition, the matrix \mathbf{W} is obtained by Gram-Schmidt orthonormalisation of the upper-triangular matrix \mathbf{r} . In performing this orthonormalisation, we have to compute the diagonal elements d_{ii} , so there is no extra work involved in correcting the \mathbf{r} if we are calculating the eigenvectors \mathbf{W} . Note that this Gram-Schmidt procedure does not represent an extra overhead in solving the system of ODEs (6.3)-(6.5), as the orthonormalisation need only be effected at the end of the integration, when the eigenvectors are required. This orthonormalisation should not be confused with the continuous Gram-Schmidt orthonormalisation of the QR method, whose purpose is to evolve the orthogonal frame given by \mathbf{Q} .

The driving term Y is

$$Y = \sum_{i=1}^n (d^{-1})_{ij} \dot{X}_j ;$$

where

$$X_{ij} = \sum_{k=1}^n Q_k \frac{\partial^2 V^k}{\partial x^i \partial x^j} ,$$

is analogous to \tilde{X} of the SVD method, and is also symmetric in i and j . The lower-triangular matrix $d^{-1} = rW$ was defined in (6.7).

In order to solve (6.12)–(6.14), we need to obtain the derivatives $W^T W_-$. Because W is obtained from r via Gram–Schmidt orthonormalisation, the time derivatives of W are deduced from those of r by differentiation of (6.9). After multiplying that equation by W_p , with $p < n$, we find

$$(W^T W_-)_{pn} = \sum_{p'=1}^{n-1} d^{-1}_{pp'} \sum_{i=1}^n W_{pi} \dot{r}_{pi} + \sum_{i=1}^{n-1} (d^{-1})_{pi} (W^T W_-)_{in} ; \quad p < n : \quad (6.15)$$

Owing to the orthogonality of W , the matrix $(W^T W_-)$ is antisymmetric. Equation (6.15) defines a recurrence relation for the $(W^T W_-)$, starting with $(W^T W_-)_1$, in terms of the time derivatives of r , given by (6.5).

The recipe for finding the Lagrangian derivatives thus consists of solving (2.1), (6.3)–(6.5) and (6.12)–(6.14) using a standard ODE integration scheme. In doing so, use must be made of the Gram–Schmidt procedure (6.9), which yields W and consequently also d via $d^{-1} = rW$. The matrix d must then be inserted into the recurrence relation (6.15) for $W^T W_-$, allowing finally the full evaluation of the right-hand side of (6.12)–(6.14). The total number of ODEs involved is $n(2n^2 + 3n + 3) = 2$; in two dimensions, this is 17, in three, 45. In evaluating the right-hand side of (6.12)–(6.14), the most expensive term to evaluate is Y , which scales as n^4 , obfuscating the cost of the Gram–Schmidt procedures for W and $W^T W_-$. It is thus clear that this numerical method is not well suited to higher-dimensional dynamical systems. However, it is appropriate to applications such as chaotic mixing, where v is a two- or three-dimensional flow.

We are not quite done yet: even though we can now solve the ODEs, they do not give the Lagrangian derivatives of the \dot{r}_p and W_q directly. The W_q are obtained from the r_p via Gram–Schmidt orthonormalisation, so we need to proceed as we did for the time derivatives of W , (6.15), and take a Lagrangian derivative of (6.9). We obtain the recurrence relation

$$\dot{W}_{pq} = \sum_{p'=1}^{n-1} d^{-1}_{pp'} \sum_{i=1}^n W_{pi} \dot{r}_{pi} + \sum_{i=1}^{n-1} (d^{-1})_{pi} \dot{W}_{in} ; \quad p < n ; \quad (6.16)$$

where

$$\dot{r}_{pi} = \sum_{q=1}^n W_{qi} \dot{r}_q = \sum_{q=1}^n W_{qi} \frac{\partial W_p}{\partial a^q}$$

is the analogue to λ_1 in the SVD method. The recurrence relation is solved by first evaluating λ_1 and then incrementing n , always keeping $\lambda_n < \lambda_{n-1}$. The antisymmetry of λ_n in n and m means that we do not need to consider the $\lambda_n > \lambda_{n-1}$ case.

Finally, we need the Lagrangian derivative of d in order to find the derivative of λ_n . Indeed, because of the correction to d given in (6.8), we have

$$\lambda_n = \frac{1}{d} \frac{\partial \log d}{\partial a^n};$$

where λ_n was defined in (4.8), and

$$\lambda_n = \frac{1}{d} \frac{\partial \log d}{\partial a^n}$$

is the correction. The explicit form for λ_n is readily obtained in the same manner as (6.16) by differentiating (6.10), to yield

$$\lambda_n = \frac{1}{d} \frac{\partial \log d}{\partial a^n} = \frac{1}{d} \frac{\partial \log d}{\partial a^n} = \frac{1}{d} \frac{\partial \log d}{\partial a^n} \quad (6.17)$$

Equation (6.17) is the same as (6.16) with $\lambda_n = \lambda_n$, so that numerically both λ_n and λ_n can be obtained in the same loop.

This completes the numerical procedure. As we mentioned in section 6.1, there is no real additional numerical burden involved in evaluating (6.16) and (6.17), as the Lagrangian derivatives of W and d are not needed to solve the ODEs. These derivatives can be calculated as desired, either at regular intervals or at the end of the integration.

There are two related but distinct numerical problems when finding the Lagrangian derivatives. The first is that the direction of fastest stretching of the flow dominates and must be isolated from the other directions, otherwise it quickly becomes impossible to extract subdominant directions because of lack of numerical precision. This is the problem we have solved with our method, by projecting along appropriate characteristic axes. The second numerical problem is that the exponentially growing quantities in the method eventually lead to numerical overflow (or underflow for exponentially decreasing quantities). In the QR method for the coefficients of expansion, (6.3) can easily be rewritten as an equation for $\log d$, replacing the exponential behaviour by linear growth (or decay) in time. The same cannot be done in (6.12)–(6.14) because the rescaling of the driving term introduces a large damping term that makes the system extremely stiff (because the rescaling itself is time-dependent). But overflowing only becomes a problem if we solve the system for very long times (on the timescales necessary for the Lyapunov exponents to converge).

A final note on the stability of the algorithm: in Refs. [23] and [35] it is shown that the numerical integration of the orthogonal matrix Q is unstable (the matrix loses orthogonality), unless the full spectrum of eigenvalues is calculated, in which case the algorithm is neutrally stable. Since we always assume we are computing the full spectrum, the stability of Q is not a concern.

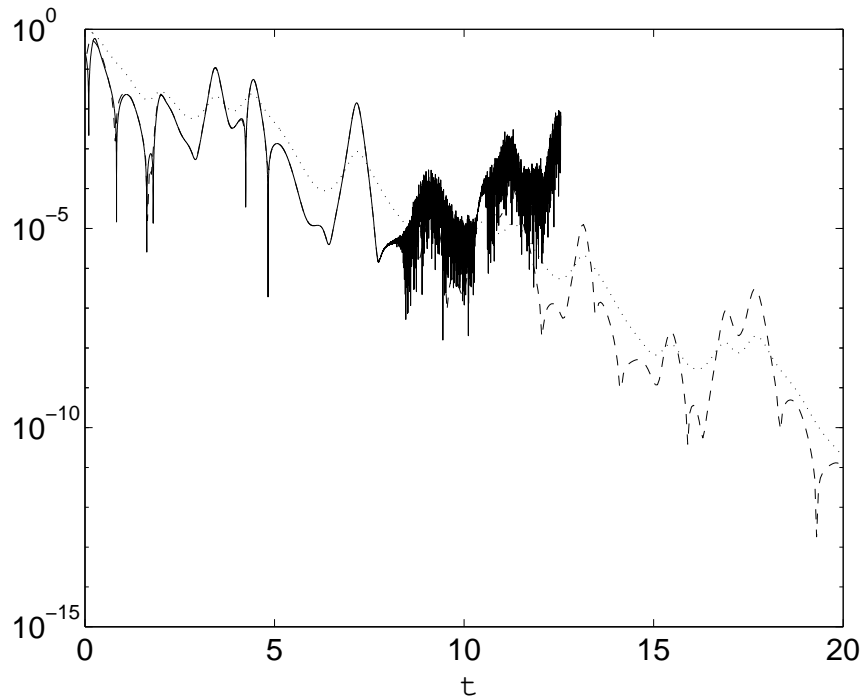


Figure 1. The type I constraint given by (5.13), for the ABC flow with $A = B = 5$, $C = 2$, computed with the direct method of section 3 (| |) and with the QR method of section 6 ({ {). The direct method becomes unreliable after $t = 7$ due to roundoff error. The QR method unambiguously exhibits the convergence of the constraint to zero, which agrees well with the predicted convergence rate λ_3 ().

6.3. Numerical Verification of Constraints

In figure 1, the type I constraint given by (5.13) is shown for the ABC flow with $A = B = 5, C = 2$ [11]. (These parameter values give a large chaotic region and make the convergence of the constraints faster, but the constraints are also satisfied for the more usual values $A = B = C = 1$.) The constraint is computed with the direct method of section 3 and with the QR method of section 6. It would be difficult to make a case for the constraint converging to zero based on the direct method: the noise starting at $t = 7$ reflects the effects of limited numerical precision inherent to the method as the elements of M become exponentially large. The QR method, however, has the constraint reaching 10^{-12} before precision problems set in (this is not a flaw in the method: the terms in (5.13) cannot cancel beyond the number of digits of precision represented by the machine). The constraint is predicted by (5.13) to converge as λ_3 , which is also shown in figure 1.

Figure 2 shows a plot of the type II constraint given by equation (5.19), also for the ABC flow. The constraint converges as $(\lambda_2 - \lambda_1)^2$, as predicted by (5.15). The same comments as for figure 1 apply regarding numerical precision.

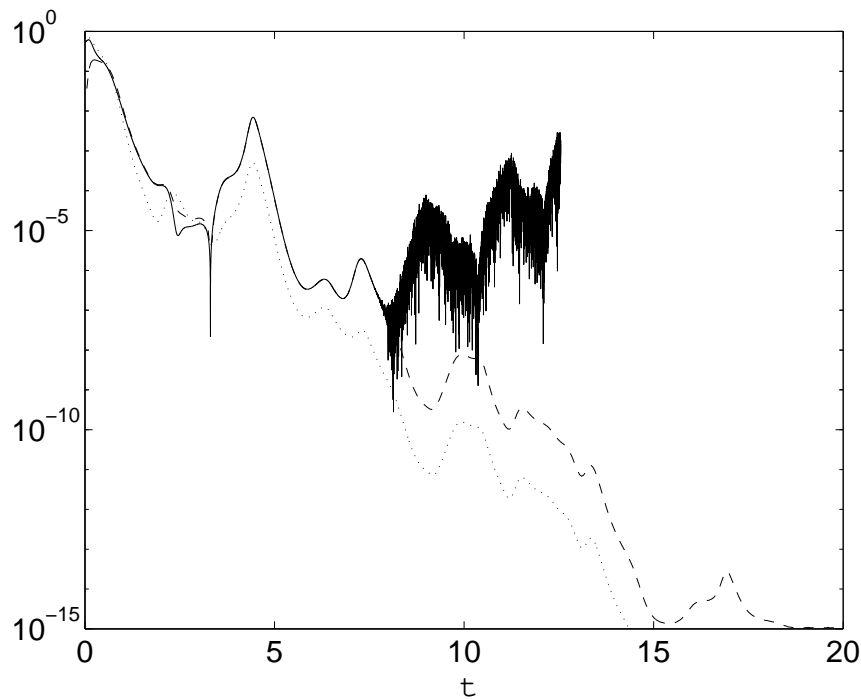


Figure 2. The type II constraint $\mathcal{P}_1 = \mathbf{r}_0 \cdot \hat{\mathbf{e}}_1$ [equation (5.19)] for the ABC flow with $A = B = 5, C = 2$, computed with the direct method of section 3 (—) and with the QR method of section 6 (---). The direct method becomes unreliable after $t \approx 7$ due to round-off error. The QR method clearly illustrates the convergence of $\mathcal{P}_1 = \mathbf{r}_0 \cdot \hat{\mathbf{e}}_1$ to zero, at the predicted rate of $(\lambda_2 - 1)^2$ (—).

7. Discussion

Lagrangian coordinates can greatly simplify the form of partial differential equations, especially equations of an advective nature. We have taken the viewpoint that to fully characterise quantities expressed in the Lagrangian frame it is necessary to know how to compute derivatives with respect to these Lagrangian coordinates. This amounts to understanding how the Lagrangian frame itself (as defined by the characteristic eigenvectors and the coefficients of expansion) vary under small changes of initial conditions. Obtaining such derivatives with accuracy is difficult in chaotic flows because the stretching rates of phase-fluid elements vary greatly along different directions.

The Lagrangian derivatives can be computed by differentiating existing methods for finding Lyapunov exponents and eigenvectors. Direct differentiation of the equations of motion is useful only for short times. For long times limited numerical precision becomes problematic and a decomposition method is needed. The SVD method proved useful in deriving the asymptotic form of the Lagrangian derivatives and in deriving differential constraints. The singularities possessed by the SVD method and its large number of components make its use in numerical computations difficult. The QR decomposition method is more appropriate for numerical implementations, but is less transparent than the SVD method. We used the QR method to accurately verify the differential

constraints derived in the paper.

The techniques described here apply only to the first derivatives of the various quantities, which actually depend on the second derivatives of the vector field. First derivatives are sufficient for the study of many systems, including the advection-diffusion equation and the dynamo problem. This seems paradoxical because both the advection-diffusion equation and the resistive magnetic induction equation involve second derivatives in space, but when transformed to Lagrangian coordinates the equation only involves first derivatives of the metric tensor g [6,12]: the second derivatives are only applied to the initial data.

The results derived in the Lagrangian frame can easily be adapted to the Eulerian picture with only minor modifications. The crux of the difference lies in holding the Eulerian initial condition fixed, and integrating the initial condition backwards in time. The translation between the Eulerian and Lagrangian pictures is outlined in Appendix C.

Some of the differential constraints derived in this and earlier papers have been applied to the study of the advection-diffusion equation [6,12,31]. In particular, in Ref. [12] a type I constraint (Section 5.2.1) is used to obtain an effective one-dimensional diffusion equation for chaotic flows. In Ref. [36] the Eulerian form of the type I constraint, equation (C.5), is used to derive a power-law relationship between the curvature of a material line and the amount of stretching the line has undergone. This same constraint is used in [8,9] to derive an invariant measure of the spatial length distribution of material lines in two dimensions. Finally, in Ref. [37] a type II constraint (Section 5.2.2) is used to show that the onset of dissipation in the kinematic dynamo occurs much later than a straightforward estimate indicates. This is because the leading-order behaviour of the power dissipation (Ohmic heating) in the dynamo is proportional to a type II constraint, so it does not grow as fast as expected.

The behaviour of second and higher derivatives has not been investigated. Whilst in principle the method could be extended to cover such cases, the complexity of the calculation and the smoothness requirements on v are prohibitive. A study of the consequences of the degeneracy of Lyapunov exponents—as occurs for instance in Hamiltonian systems—remains to be done.

Acknowledgements

The author thanks Allen H. Boozer and David Lazanja for helpful discussions. This work was supported by an NSF/DOE Partnership in Basic Plasma Science grant, No. DE-FG 02-97ER 54441.

Appendix A. Asymptotic Behaviour of the Lagrangian Derivatives

In this appendix we use the equations of motion (4.9)–(4.11) to derive the asymptotic behaviour (4.13)–(4.15) of the Lagrangian derivatives, as defined by (4.8).

For $\epsilon < 1$, assuming $\epsilon < 1$, the last term in (4.10) is

$$\sum_q V_q \frac{\partial}{\partial a^q} (U^T U) = \sum_q V_q \frac{\partial \mathcal{G}}{\partial a^q} \sum_q \epsilon^2 V_q \frac{\partial \mathcal{G}}{\partial a^q} + 2 \epsilon^2 \mathcal{A} \quad (A.1)$$

The first term in (A.1) is

$$\sum_q V_q \frac{\partial \mathcal{G}}{\partial a^q} = \sum_q \mathcal{X} + \sum_q \mathcal{G} + \sum_q \mathcal{G} : \quad (A.2)$$

This shows that the second term in (A.1) can be neglected compared to the first because it is smaller by a factor ϵ^2 . We also neglect the third term, which couples \mathcal{X} and \mathcal{G} (it is straightforward to go back and check that the neglect is justified).

After these approximations, the evolution equation for \mathcal{X} is

$$\dot{\mathcal{X}} = \sum_q V_q \frac{\partial}{\partial a^q} (U^T U) \mathcal{X} + \sum_q V_q \frac{\partial}{\partial a^q} (U^T U) \mathcal{G} + \sum_q V_q \frac{\partial}{\partial a^q} (U^T U) \mathcal{G} + \sum_q V_q \frac{\partial}{\partial a^q} (U^T U) \mathcal{X} ; \quad (A.3)$$

for $\epsilon < 1$. This is a linear system in \mathcal{X} , with nonconstant coefficients and a driving term given by \mathcal{G} . The only term that couples \mathcal{X} 's with \mathcal{G} is the $V^T V$ one, which is small compared to $U^T U$. We neglect this term (again, after the fact it is easy to check that the neglect is consistent), and rearrange (A.3) to give

$$\dot{\mathcal{X}} = (\mathcal{G} - \mathcal{G}) + \sum_q \mathcal{A} \mathcal{X} + \sum_q \mathcal{A} \mathcal{G} \mathcal{X} : \quad (A.4)$$

Let us ignore the driving term for now and consider the homogeneous solution \mathcal{X}^h . Through a judicious ordering of the \mathcal{A} that gives the linear part of (A.4) a triangular structure, it can be shown that \mathcal{X}^h is bounded. If we assume that the motion of the system takes place in a bounded region of phase space, \mathcal{X} is also bounded (we also assume that v is twice differentiable and that its second derivative is Lipschitz). Then the inhomogeneous driving term \mathcal{X} asymptotically goes as ϵ . (A similar argument was used in section 4.1 to show convergence of V .) Asymptotically, then, in (A.4) either the exponentially decaying linear part or the driving term dominates, depending on which has the larger growth rate. We conclude that

$$\mathcal{X} = \max(\epsilon; \epsilon) e^{-\lambda t} ; \quad t \gg 1; \quad (A.5)$$

where $e^{-\lambda t}$ is some function that neither grows nor decays exponentially.

Next, we investigate the asymptotic behaviour of \mathcal{G} . Its time evolution is given by (4.9), which after inserting our asymptotic solution for \mathcal{X} becomes

$$\dot{\mathcal{G}} = \sum_q V_q \frac{\partial}{\partial a^q} (V^T V) \mathcal{G} + \max(\epsilon; \epsilon) \text{drive};$$

where drive is some non-exponential function. Notice that \mathcal{G} 's with \mathcal{G} are uncoupled. The matrix $V^T V$ has elements that are decreasing exponentially, so we can solve the system perturbatively. The solution, valid to first-order in $V^T V$, is of the form

$$\mathcal{G} = \max(\epsilon; \epsilon) e^{-\lambda t} + \epsilon ; \quad t \gg 1: \quad (A.6)$$

where the time dependence of $e^{\lambda t}$ is non-exponential.

Finally, having derived an asymptotic form for \dot{y} and \ddot{y} , we can do the same for the Lagrangian derivatives of V , as embodied by [Equation (4.8)]. For $\epsilon < 1$, assuming $\epsilon \ll 1$, we write (4.11) for \dot{V} in the approximate form

$$\begin{aligned} -\ddot{V} &= \sum_{i=1}^N \lambda_i^2 (V^T V)_i + (V^T V)_{drive} \\ &+ \max(\lambda_1^2; \lambda_2^2; \lambda_3^2) e^{\lambda_{drive} t}; \end{aligned} \quad (A.7)$$

where $drive$ is a term with possible time dependence but without exponential behaviour. The matrix $V^T V$, given in (4.5), becomes exponentially small with time. We can thus solve (A.7) perturbatively, yielding

$$= \max(\lambda_1^2; \lambda_2^2; \lambda_3^2) e^{\lambda_{drive} t} + \epsilon^2; \quad t \gg 1; \quad (A.8)$$

where the time dependence of $e^{\lambda t}$ is non-exponential.

A comment about the perturbation expansions in small $V^T V$ used to obtain (A.6) and (A.8) is in order. For a small parameter ϵ , a perturbative expansion solution to an equation of the form

$$\ddot{y} = \epsilon y +$$

is valid only for $\epsilon t \ll 1$. So for large time, at fixed ϵ , the solution must eventually become invalid. However, in our case the parameter ϵ , corresponding to $V^T V$, actually decreases exponentially in time (for nondegenerate eigenvalues λ_i). Thus, $\epsilon t \ll 1$ even for large t , and the expansion remains valid.

Appendix B. The Eigenvalues of g and the QR Method

In this appendix we prove that (6.8) gives the asymptotically correct value of the eigenvectors \hat{e} and coefficients of expansion ϵ (the square root of the eigenvalues of g). This result was shown in Ref. [24]. We present here a different proof, proceeding by induction and deriving the eigenvectors and eigenvalues together.

Let d be the lower-triangular matrix that performs the Gram-Schmidt orthonormalisation of r , that is

$$W^T = d r; \quad (B.1)$$

where d is lower-triangular and W is orthogonal (this is simply (6.7) in matrix form). The matrix d is nonsingular, so we can invert (6.7) and write $r = d^{-1} W^T$.

Using the definition of the metric, $g = M^T M$, and the QR decomposition (6.1), we have

$$g W = W F; \quad \text{where } F \equiv (d^{-1})^T D^2 (d^{-1}); \quad (B.2)$$

If F were diagonal, then we would be done; the matrix F is not diagonal, but we show that it can be made so by exponentially small corrections of the W .

Writing out F explicitly, we find

$$F = \sum_{n=0}^{\infty} (d^{-1})^{n+2} (d^{-1})^n : \\ = \max(\cdot) :$$

The $\max(\cdot)$ is the lower bound of the sum owing to the lower-triangular form of d . Looking at (6.5), it is clear the terms converge to constant values, because for $\lambda > 0$, $\lambda^n \rightarrow 0$ exponentially in time. Hence, by their definition, W and d also converge to constant values in time. All of the exponential behaviour is thus embodied in d . Keeping only the dominant term, we have

$$F \approx (d^{-1})^{n+2} (d^{-1})^n : \\ = \max(\cdot) :$$

Note that since d is triangular we have $(d^{-1})^{n+2} = d^{-1}$. For the first column of W , it follows that

$$\sum_q g_{pq} W_{q1} = \sum_p W_p F_{p1} + \frac{1}{d_{11}^2} W_{p1} ;$$

showing that the first column of W is an eigenvector of g with eigenvalue $(\lambda_1 = d_{11})^2$. Let

$$W_p^0 = W_p + \sum_{n=1}^{\infty} \frac{d^2}{2} F^n W_p ; \quad (B.3)$$

which represents an exponentially small correction to the matrix element W_p , because $F^n \approx d^{2n}$ for $\lambda < 1$. Assume that the columns W_q^0 , $\lambda_q < 1$, are eigenvectors of g with eigenvalue $(\lambda_q = d_{11})^2$. We show by induction that with the (small) correction (B.3) the column W_q^0 is an eigenvector of g with eigenvalue $(\lambda_q = d_{11})^2$.

Using $F = W^T g W$ and (B.3), the corrected matrix element F^0 , with $\lambda_q < 1$, is

$$F^0 = W_p^0 g_{pq} W_q = F + \sum_{n=1}^{\infty} \frac{d^2}{2} F^n F ; \quad \lambda_q < 1 :$$

We use the induction hypothesis that $F^n = (\lambda_q = d_{11})^{2n}$ when both p and q are less than n , and find

$$F^0 = F + \sum_{n=1}^{\infty} \frac{d^2}{2} F^n \frac{d^2}{d^2} = F + F = 0 ;$$

to exponential accuracy. The corrected diagonal element F^0 is

$$F^0 = F + \sum_{n=1}^{\infty} \frac{d^2}{2} F^n F + \sum_{n=1}^{\infty} \sum_{m=1}^{\infty} \frac{d^2}{2} \frac{d^2}{2} F^n F^m F \\ = F + \sum_{n=1}^{\infty} \frac{d^2}{2} F^{2n} , \quad F \quad (B.4)$$

to leading order. Thus, to exponential accuracy W_q^0 is indeed an eigenvector of g with eigenvalue $F = (\lambda_q = d_{11})^2$.

To complete the proof, we need to show that the columns W_q , with $q > 1$, are not modified by the correction (B.3). We have

$$F^0 = F + \sum_{q=1}^{X-1} \frac{d^2}{2} F^{(q)} F^{(q)}; \quad \lambda_q > 0;$$

which to leading order is

$$F^0 = (d^{-1})^{(1)} (d^{-1})^{(2)} + O\left(\frac{d^2}{2^{X-1}}\right)^2, \quad F^{(q)};$$

showing that the correction can be neglected.

We have thus proved by induction that the correction (B.3) to W makes F diagonal to leading order, leaving its diagonal elements unaffected. However, the correction (B.3) is of order $(d^{-1})^2$, which is exponentially small with time. We conclude that the eigenvectors of g and corresponding coefficients of expansion are

$$(\hat{e})_q = W_q; \quad \lambda_q = \frac{1}{d};$$

to exponential accuracy with time. The relative error on \hat{e} and λ^2 is of order $(d^{-1})^2$, as can be seen from the leading-order correction in (B.3) and (B.4).

Appendix C. The Eulerian Perspective

The results derived in the paper regarding Lagrangian derivatives can readily be adapted to an Eulerian framework. The Lagrangian derivatives can be regarded as measuring the effect of an infinitesimal change in the initial condition of a trajectory. Conversely, one can regard Eulerian derivatives as the effect of an infinitesimal change in the final condition of a trajectory, with the integration being performed backwards in time. This is the viewpoint taken in studies of the alignment of material lines with the Eulerian unstable manifold of a system, a phenomenon referred to as asymptotic directionality [8,9,22,38,39].

In our framework, the Eulerian characteristic directions are computed from the metric

$$h^{ij}(t; t_0; x) = \sum_{p=1}^{X^n} M_p^i M_p^j; \quad (C.1)$$

or $h = M M^T = g^T$. We have explicitly written the dependence on initial time because we are now interested in evolving t_0 towards -1 , whilst holding the Eulerian coordinates t and x fixed. The dynamical system (2.1) and the SVD equations (4.2)–(4.4) are also evolved backwards in time: the method yields M^{-1} , so that we must take the inverse of the resulting h to obtain the "forward-time" coefficients of expansion. We assume the forward-time coefficients have then been reordered in the usual decreasing manner, so that λ_1 is still the fastest-growing coefficient (the columns of U and V are also reordered). The asymptotic behaviour of the Eulerian derivatives will thus be the inverse of their Lagrangian counterpart. The columns of V now contain vectors

associated with the Eulerian frame. The relevant Eulerian definitions corresponding to (4.8) simply involve replacing $\partial=\partial_a$ by $\partial=\partial_x$ to reflect the fact the derivatives are now taken with respect to the Eulerian coordinates. Their asymptotic behaviour is

$$\lambda_1^E = \max \lambda_1^E; \quad e^E; \quad (C.2)$$

$$\lambda_2^E = \max \lambda_1^E; \quad e^E + \lambda_1^E; \quad (C.3)$$

$$\lambda_3^E = \max \lambda_1^E; \quad e^E + \lambda_1^E; \quad (C.4)$$

where the ^E superscript reminds us that these are Eulerian quantities. The discussion of the Hessian and constraints in section 5 is the same for the Eulerian derivatives, except that the coefficients of expansion corresponding to contracting directions are replaced by the inverse of those of the expanding directions. For instance, the type I constraint given by (5.13) becomes

$$\sum_i^X \lambda_j^{j=2} \frac{\partial}{\partial x^i} \lambda_j^{j=2} (e_1^E)_i + \sum_i^X (e_1^E)_i \frac{\partial}{\partial x^i} \log \lambda_1^E = \max \lambda_1^E; \quad \frac{2}{11} \neq 0; \quad (C.5)$$

This is a more general form of the relation derived for the 2D incompressible case in Refs. [8,9], used to derive an invariant measure of the spatial length distribution of material lines.

References

- [1] J.Guckenheimer and P.J.Holmes, *Nonlinear Oscillations, Dynamical Systems, and Bifurcations of Vector Fields* (Springer-Verlag, New York, 1983).
- [2] V.I.Arnold, *Ordinary Differential Equations*, Third ed. (Springer-Verlag, Berlin, 1992).
- [3] J.-P.Eckmann and D.Ruelle, *Rev. Modern Phys.* 57, 617 (1985).
- [4] A.M.Lyapunov, *The General Problem of the Stability of Motion* (Taylor & Francis, London, 1992), English translation. First published in Russian in 1892 by the Mathematical Society of Khar'kov.
- [5] A.H.Boozer, *Astrophys.J.* 394, 357 (1992).
- [6] X.Z.Tang and A.H.Boozer, *Physica D* 95, 283 (1996).
- [7] X.Z.Tang and A.H.Boozer, *Phys. Plasmas* 7, 1113 (2000).
- [8] M.Giona and A.Adrover, *Phys.Rev.Lett.* 81, 3864 (1998).
- [9] A.Adrover and M.Giona, *Phys.Rev.E* 60, 347 (1999).
- [10] L.D.Landau and E.M.Lifschitz, *Fluid Mechanics, Course of Theoretical Physics Vol. 6*, Second ed. (Butterworth-Heinemann, Oxford, U.K., 1998).
- [11] S.Childress and A.D.Gilbert, *Stretch, Twist, Fold: The Fast Dynamics* (Springer-Verlag, Berlin, 1995).
- [12] J.-L.Thieault, Preprint (2001), nlin.CD/0105026.
- [13] U.Dressler and J.D.Farmer, *Physica D* 59, 365 (1992).
- [14] T.J.Taylor, *Nonlinearity* 6, 369 (1993).
- [15] G.K.Batchelor, *Proc.R.Soc.Lond.A* 213, 349 (1952).
- [16] S.B.Pope, *Int.J.Engng.Sci.* 26, 445 (1988).
- [17] S.B.Pope, P.K.Yeung, and S.S.Girimaji, *Phys.Fluids A* 1, 2010 (1989).
- [18] S.S.Girimaji, *Phys.Fluids A* 3, 1772 (1991).
- [19] I.T.Drummond and W.Munch, *J.Fluid Mech.* 225, 529 (1991).
- [20] M.Liu and F.J.Muzzio, *Phys.Fluids* 8, 75 (1996).
- [21] D.M.Hobbs and F.J.Muzzio, *Phys.Fluids* 10, 1942 (1998).

- [22] S. Cerbelli, J.M. Zalc, and F.J. Muzzio, *Chem. Eng. Sci.* 55, 363 (2000).
- [23] J.M. Greene and J.S. Kin, *Physica D* 24, 213 (1987).
- [24] I. Goldhirsch, P. Sulem, and S.A. Orszag, *Physica D* 27, 311 (1987).
- [25] J.-L. Thieault and A.H. Boozer, *Chaos* 11, 16 (2001).
- [26] K. Geist, U. Parlitz, and W. Lauterborn, *Prog. Theoret. Phys.* 83, 875 (1990).
- [27] G. Benettin, L. Galgani, and J.-M. Strelcyn, *Phys. Rev. A* 14, 2338 (1976).
- [28] I. Shimada and T. Nagashima, *Prog. Theoret. Phys.* 61, 1605 (1979).
- [29] J.M. Ottino, *The Kinematics of Mixing: Stretching, Chaos, and Transport* (Cambridge University Press, Cambridge, U.K., 1989).
- [30] V.I. Oseledec, *Trans. Moscow Math. Soc.* 19, 197 (1968).
- [31] X.Z. Tang and A.H. Boozer, *Phys. Fluids* 11, 1418 (1999).
- [32] X.Z. Tang and A.H. Boozer, *Chaos* 9, 183 (1999).
- [33] B. Schutz, *Differential Geometry* (Cambridge University Press, Cambridge, U.K., 1980).
- [34] R.M. Wald, *General Relativity* (University of Chicago Press, Chicago, 1984).
- [35] F. Christiansen and H.H. Rugh, *Nonlinearity* 10, 1063 (1997).
- [36] J.-L. Thieault, Preprint (2002), [nlin.CD/0204069](#).
- [37] J.-L. Thieault and A.H. Boozer, Preprint (2002), *Phys. Plasmas*, in submission, [nlin.CD/0209042](#).
- [38] M. Giona, A. Adrover, F.J. Muzzio, and S. Cerbelli, *Physica D* 132, 298 (1999).
- [39] M. Giona, A. Adrover, F.J. Muzzio, and S. Cerbelli, *Chem. Eng. Sci.* 55, 381 (2000).